Ab initio characterization of the giant magnetoresistance in realistic spin valves

P. Weinberger
Center for Computational Materials Science, Technische Universität Wien, Getreidemarkt 9/158, 1060 Vienna, Austria

L. Szunyogh
Center for Computational Materials Science, Technische Universität Wien, Getreidemarkt 9/158, 1060 Vienna, Austria
and Department of Theoretical Physics, Budapest University of Technology and Economics Budafoki út. 8, 1521 Budapest, Hungary
(Received 9 July 2002; published 31 October 2002)

The electric transport properties of a rather complicated spin-valve system containing NiFe permalloy, CoFe hard magnets and two types of spacers (Cu,Ru) are investigated theoretically in terms of the relativistic spin-polarized versions of the Screened Korringa-Kohn-Rostoker method and the Kubo-Greenwood equation. It is found that the regimes of antiferromagnetic coupling relevant for the giant magnetoresistance (GMR) are mostly determined by the thickness of the Cu-spacer: the nodes of oscillation of the interlayer exchange coupling (IEC) with respect to the Cu-spacer thickness are shifted only marginally by the presence of a very thin Ru cap. Also found are oscillations of the IEC and GMR with respect to the thickness of the hard magnet parts of the system (CoFe) and with respect to the Ru-spacer thickness. Viewed with respect to the thickness of the Cu-spacer the minima in and the actual value of the giant magnetoresistance as a function of the thickness of the Ru-spacer are in rather good agreement with experiment.

DOI: 10.1103/PhysRevB.66.144427 PACS number(s): 75.70.Ak, 75.30.Gw, 75.70.Cn

I. INTRODUCTION

Giant magnetoresistance (GMR) devices seem to be used now in many fields of application; they are still considered to be *the* mayor outcome of research in ''spintronics.'' The actual composition of such devices, however, can be fairly complicated and results from ''chemical kitchen'' experience in producing relevant layered systems. Very often GMR devices contain several ingredients such as soft and hard magnetic parts, more than one spacer material, and an antiferromagnetic part serving as pinning material. In spite of all theoretical efforts[1] with all these components it is usually not possible to trace what kind of effect is induced from what part of the system. In the present paper a typical spin-valve system of this kind consisting of a NiFe permalloy soft magnet, CoFe hard magnets, and Cu and Ru spacers is analyzed in theoretical terms by considering the interlayer exchange coupling (IEC) and the GMR of the various parts of such a system. Such a partitioning of a given system is of course only possible theoretically and is meant to give a better insight into some rules of thumb based on chemical experience.

The actual experimental sample[2] underlayer [55 Å]|NiFe[10 Å]|CoFe[x Å]|Cu[y Å]|CoFe[x Å]|Ru[4 Å]|CoFe [x Å]|IrMn[70 Å]| overlayer[55 Å] was grown on 3000 Å of SiO_2, for the overlayer a thick cap of Ta is used. In here it is modeled theoretically by considering the permalloy (NiFe) slab as substrate and replacing the artificial antiferromagnetic (AF) part consisting of IrMn layers and the overlayer by vacuum. It should be noted that this particular replacement corresponds to the use of a reflecting boundary condition as easily as can be seen from Fig. 2 of Ref. 3. Clearly enough the main purpose of using an AF part in a spin-valve system is the pinning effect, by which, however, the actual giant magnetoresistance ratio remains unaffected: the AF part of the system governs mainly the size of a possibly present exchange bias.[4]

In order to sort out the effect of the thickness of the Cu spacer, of the Ru spacer, and of the slabs of the hard magnets, four partial systems are considered (systems A–D, see Table I) with system D reflecting closely the experimental sample. The actual compositions of permalloy and of the CoFe alloy, which were not mentioned in Ref. 2, were communicated by Seigler.[5] Quite clearly not all thickness param-

TABLE I. Partial systems (1 ML corresponds to 2.0488 Å).

System A		System B	
Thickness (ML)	fcc(111)	Thickness (ML)	fcc(111)
∞	$Ni_{80}Fe_{20}$	∞	$Ni_{80}Fe_{20}$
6	$Ni_{80}Fe_{20}$	6	$Ni_{80}Fe_{20}$
5	$Co_{90}Fe_{10}$	5	$Co_{90}Fe_{10}$
$2 \leqslant n \leqslant 12$	Cu	$2 \leqslant n \leqslant 12$	Cu
5	$Co_{90}Fe_{10}$	5	$Co_{90}Fe_{10}$
	vacuum	2	Ru
			vacuum
System C		System D	
Thickness (ML)	fcc(111)	Thickness (ML)	fcc(111)
∞	$Ni_{80}Fe_{20}$	∞	$Ni_{80}Fe_{20}$
6	$Ni_{80}Fe_{20}$	6	$Ni_{80}Fe_{20}$
5	$Co_{90}Fe_{10}$	5	$Co_{90}Fe_{10}$
5	Cu	5	Cu
$5 \leqslant m \leqslant 12$	$Co_{90}Fe_{10}$	5	$Co_{90}Fe_{10}$
	vacuum	$1 \leqslant p \leqslant 8$	Ru
		5	$Co_{90}Fe_{10}$
			vacuum

 ©2002 The American Physical Society

eters can be varied in a theoretical study simultaneously, the results, however, will show that this is indeed also not really necessary.

II. THEORETICAL AND COMPUTATIONAL DETAILS

The fully relativistic spin-polarized screened Korringa-Kohn-Rostoker method for layered systems[6] is applied within the framework of the coherent potential approximation[7] in order to calculate the electronic structure and magnetic properties of relevant parts of the spin-valve system described in detail in Table I. In all calculations an fcc-parent lattice[8] is assumed with a lattice spacing a_0 of 6.7060 a.u. (bulk fcc $Ni_{80}Fe_{20}$), i.e., no layer relaxation is considered, and six $Ni_{80}Fe_{20}$ layers serve as buffer to a semi-infinite $Ni_{80}Fe_{20}$ substrate[9,10]. In order to determine self-consistently within the local-density approximation the effective[11] potentials and effective exchange fields a minimum of 45 $\mathbf{k}_\parallel$ points in the irreducible wedge of the surface brillouin zone (ISBZ) is used. All self-consistent calculations refer to a ferromagnetic configuration with the orientation of the magnetization pointing along the surface normal; all interlayer exchange energies are evaluated at zero temperature in terms of the magnetic force theorem via an integration in the upper half of the complex energy plane along a contour which starts at a real energy well below the valence band and ends at the Fermi energy. For these calculations a total of 990 $\mathbf{k}_\parallel$ points in the ISBZ is used, which—as was shown[6] in the case of magnetic anisotropy energies—guarantees well converged results. All electric transport calculations are performed in terms of the fully relativistic spin-polarized form of the Kubo-Greenwood equation for layered systems[3,7,12,13] by using a complex Fermi energy and 1830 $\mathbf{k}_\parallel$ points in the ISBZ for the SBZ integrals, and by continuing the thus obtained resistivities numerically to the real energy axis. It should be noted that the IEC and the current-in-plane (CIP-) GMR are defined in the following by

$$\mathrm{IEC}(\mathcal{C}_i) = E_b(\mathcal{C}_i) - E_b(\mathcal{C}_0), \tag{1}$$

$$\mathrm{GMR}(\mathcal{C}_i) = \frac{\rho(\mathcal{C}_i) - \rho(\mathcal{C}_0)}{\rho(\mathcal{C}_i)}, \tag{2}$$

where $E_b(\mathcal{C}_i)$ refers to the grand-potential at $T=0$[6] for a particular magnetic configuration $\mathcal{C}_i$, the ρ's are resistivities, $\mathcal{C}_0$ corresponds to the parallel (ferromagnetic) reference configuration and $\mathcal{C}_i$ to a particular antiparallel (antiferromagnetic) configuration. The reason for using the so-called pessimistic definition of the GMR in Eq. (2) is simply that then this ratio is bounded by one. The difference to the other kind of definition (optimistic definition), namely relating the difference in the resistivities to $\rho(C_0)$ is usually rather small, see also the discussion in Ref. 3.

For systems $A-C$ the antiparallel configuration is simply defined by reversed orientations of the magnetization in the two magnetic slabs ($Ni_{80}Fe_{20}$ and $Co_{90}Fe_{10}$ on the one side, and $Co_{90}Fe_{10}$ on the other side). For system *D* this issue will be discussed separately. According to the definition given in Eq. (1) this implies that

$$\mathrm{IEC}(\mathcal{C}_i) = \begin{cases} >0; & \mathcal{C}_0 \ \text{prefered configuration} \\ <0; & \mathcal{C}_i \ \text{prefered configuration.} \end{cases} \tag{3}$$

If more than one antiparallel configuration has to be investigated then the largest negative $\mathrm{IEC}(\mathcal{C}_i)$ refers to the antiparallel ground-state configuration $\mathcal{C}_1$,

$$\mathrm{IEC}(\mathcal{C}_1) = \min_{\{\mathcal{C}_i\}}\{\mathrm{IEC}(\mathcal{C}_i) < 0\}. \tag{4}$$

It should be noted that experimentally the ferromagnetic configuration refers to a uniform in-plane orientation of the magnetization. However, since anisotropic effects in the resistances of Co/Cu related spin valves are rather very small indeed, see an actual calculation thereof in Ref. 3, by choosing a uniform perpendicular orientation for the ferromagnetic configuration this small deviation from the experimental situation is of no importance at all for the purposes of the present investigation.

III. RESULTS

A. Variation of the Cu-spacer thickness

The interlayer coupling field[2] in the experimental spin-valve system is characterized by nodes at 5.5, 10, 17, and about 21 Å. As can be seen from Fig. 1 the IEC of partial system *A*, see Table I, shows the typical oscillations of a magnetic trilayer that is antiferromagnetically coupled for Cu-spacer thicknesses between 4 and 10 Å, and between 15 and 21 Å, which corresponds very well indeed to those observed experimentally; a Ru-cap (system *B*) moves the nodes of oscillation only marginally.

The experimentally recorded GMR[2] increases between 5 Å and 9 Å of Cu from about 2% to about 10%, shows a substantial dip at 10 Å, increases again, has another much gentler dip at 12 Å and falls off slightly from about 11% beyond a spacer thickness of about 16 Å. In partial system A the calculated GMR vanishes at about 14 and 20 Å, and has a substantial dip at about 10 Å, see also Fig. 1, i.e., at Cu-spacer thicknesses at which the IEC turns from ferromagnetic to antiferromagnetic or vice versa. Interestingly enough in the GMR for partial system *B* the dip at 10 Å is much more pronounced than for system *A*. In both cases the position of this dip coincides with the very sharp dip in the experimental GMR, the second dip seen in experiment seems to be shifted there by about 1 ML towards smaller Cu-spacer thicknesses. The vanishing GMR (Fig. 1) at 20 Å is seen in the experimental data only as a very weak shoulder. It should be noted that contrary to experiment in the present theoretical approach the thicknesses can only be varied in steps of complete (perfect) monolayers, i.e., in steps of about 2 Å.

B. Variation of the thickness of a particular hard magnet slab

By varying for a particular given Cu-spacer thickness the thickness of the top $Co_{90}Fe_{10}$ slab (system *C*, see Table I) the IEC is characterized by pronounced oscillations with respect to the varied number of layers. This is shown in Fig. 2 for a trilayer system with 5 ML's of Cu. For this particular spacer thickness the coupling becomes stronger antiferromagnetic

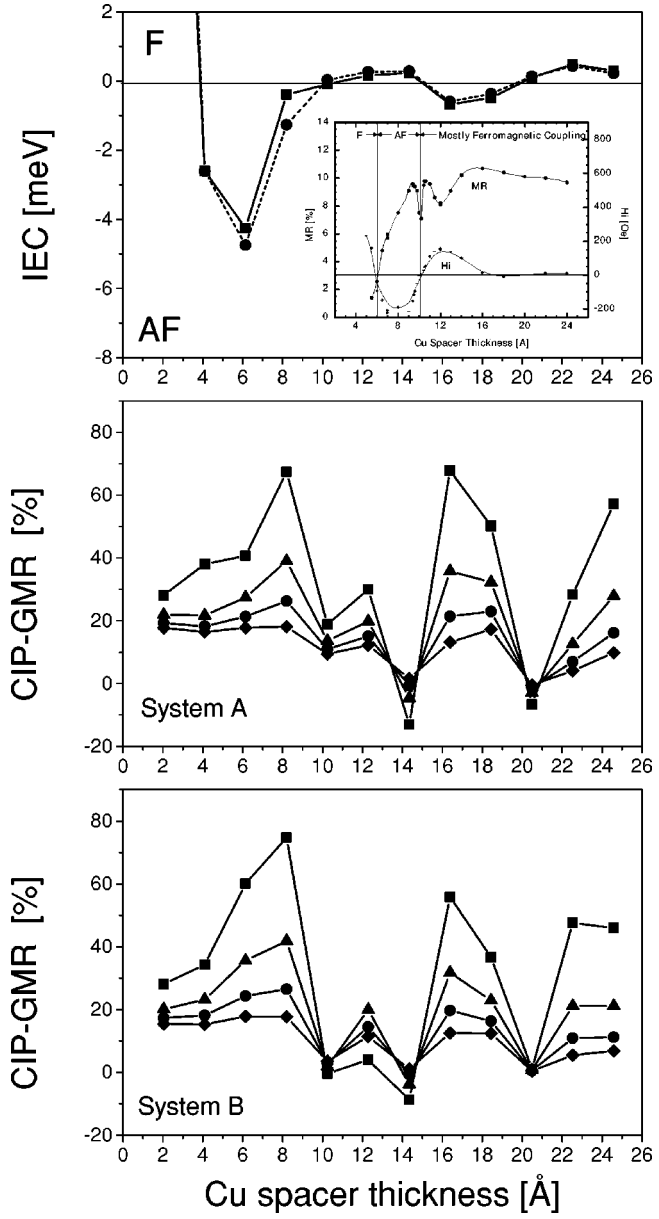

FIG. 1. IEC (top) for partial systems *A* (squares) and *B* (circles). In the GMR for system *A* (middle) and *B* (bottom) diamonds, triangles, circles, and squares refer to an imaginary part δ of the Fermi energy of 0, 1, 2, and 3 mry. The inset shows the experimental results from Ref. 2. Note that the thickness of the Cu-spacer is given in [Å], 1 ML corresponds to about 2 Å.

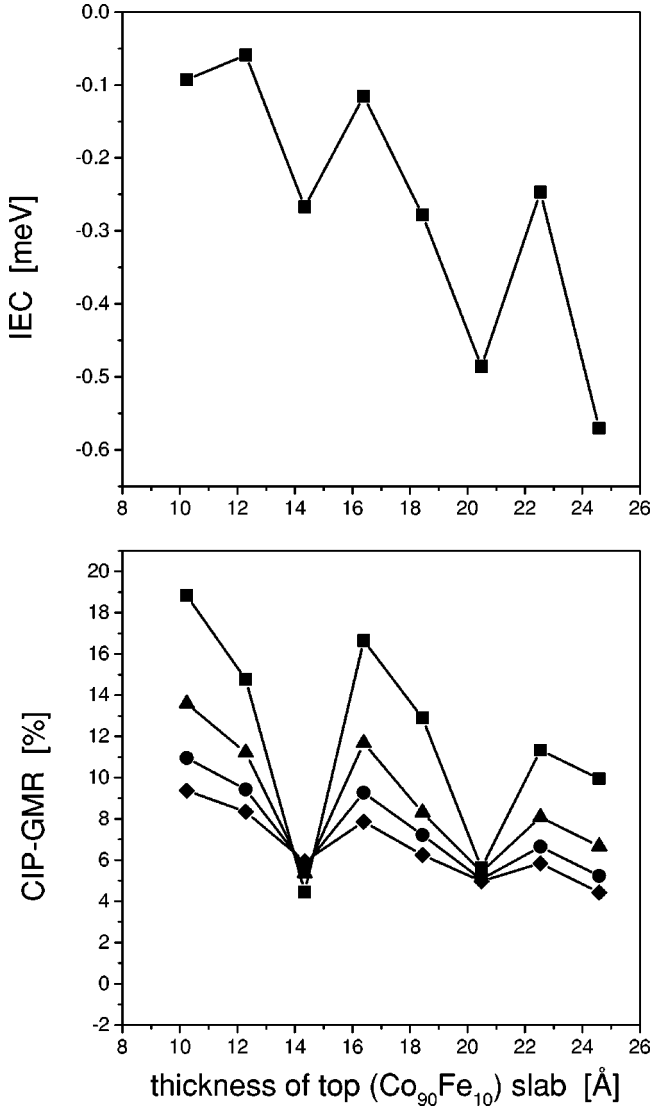

FIG. 2. IEC (top) and the GMR (bottom) of partial system *C* versus the thickness of the top $Co_{90}Fe_{10}$ magnetic slab. For the GMR squares, triangles, circles, and diamonds refer to an imaginary part δ of the Fermi energy of 0, 1, 2, and 3 mry. Note that the thickness of the $Co_{90}Fe_{10}$ slab is given in [Å], 1 ML corresponds to about 2 Å.

with increasing hard magnet thickness; the corresponding GMR (Fig. 2, bottom) exhibits the same kind of oscillations as the IEC and results into an overall decrease of the GMR with increasing thickness of the $Co_{90}Fe_{10}$ slab under investigation. These oscillations in the GMR are not to be related with switches from ferromagnetic to antiferromagnetic regimes of coupling since at the chosen Cu-spacer thickness (Fig. 2, top) all the coupling is antiferromagnetic.

It should be noted that in Figs. 1 and 2 the GMR is shown also for finite imaginary parts of the complex Fermi energy $E_F + i\delta$ since nonvanishing values of δ mimic finite temperature effects and macroscopical roughness present in the experimental samples (a value of $\delta = 2$ mry corresponds to about room temperature). For $\delta = 2$ mry the calculated GMR is in about the range of the experimentally recorded values.

In the top of Fig. 3 the actual cause for the functional form of the GMR with respect to the Cu-spacer thickness is illustrated for system *A*: in straight correlation with the *F*/AF switching, see Fig. 1, the maxima of the AF resistivity at 14 and 20 Å of Cu are even higher than the respective *F* resistivity. The lower part of this figure shows that the oscillations in the GMR with respect to the thickness of the top (right) $Co_{90}Fe_{10}$ slab displayed in Fig. 2 is induced by corresponding oscillations in the resistivity of the parallel, as well as the antiparallel configuration. Although in absolute values these oscillations are not very big, they significantly determine the oscillations in the GMR.

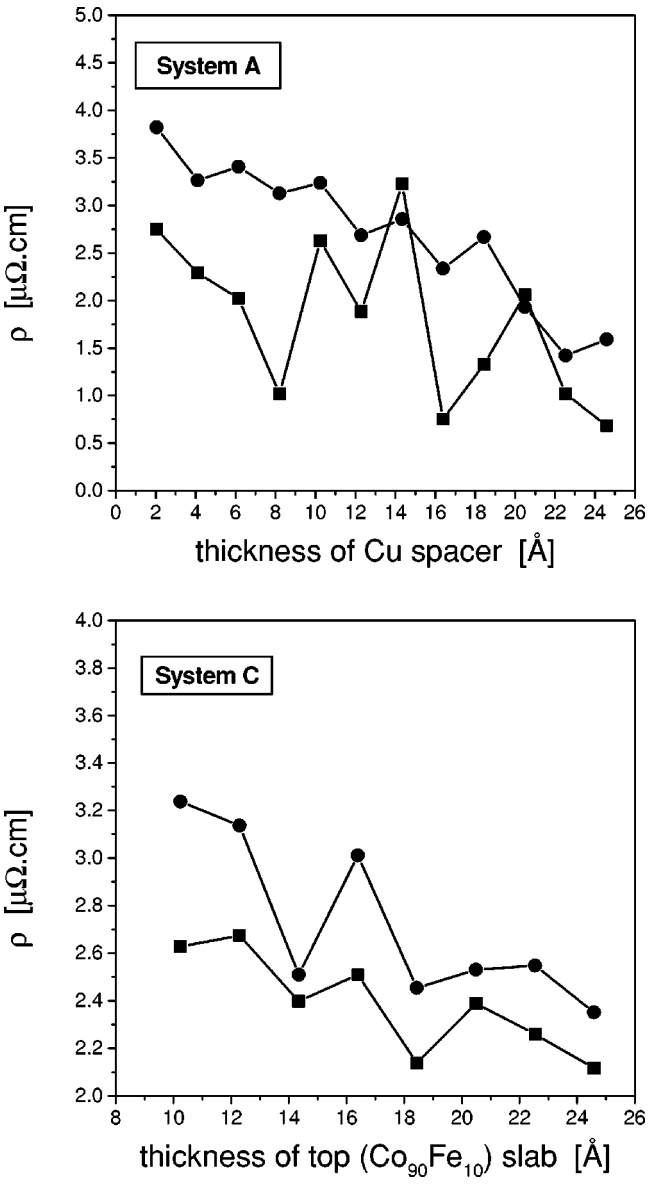

FIG. 3. Resistivities for partial systems *A* and *C* in the parallel (squares) and the antiparallel (circles) magnetic configuration versus thickness, see also Table I. Note that in both cases the thickness is given in [Å], 1 ML corresponds to about 2 Å.

C. Variations of the Ru-spacer thickness

Since in a system containing three magnetic slabs separated by two spacers a definition of the antiparallel configuration no longer is *a priori* obvious, various such configurations were assumed (see Table II) and the corresponding IEC and GMR evaluated, see also Eqs. (3) and (4). In order to understand this table correctly it is important to recall that both spacers, Cu and Ru, carry (very) small induced magnetic moments (less than $0.1\mu_B$ in the vicinity of an interface to Co), the directions of which have to be specified in a proper definition of magnetic configurations. These induced magnetic moments vanish eventually in the middle of sufficiently thick spacers.

It should be noted that configurations 1 and 2, and also in turn 3 and 4, only differ by the number of Cu layers that are additionally reversed. In Fig. 4 the IEC's for these antiparallel configurations are displayed for given thicknesses of the $Co_{90}Fe_{10}$ slabs ($m=5$, 10 Å) and the Cu spacer ($n=5$, 10 Å) as a function of the thickness of the Ru spacer. As can be seen from this figure only those configurations in which the orientations of the magnetization in the two $Co_{90}Fe_{10}$ are antiparallel (configurations 1 and 2 in Table II) show characteristic oscillations with respect to the Ru-spacer thickness; energetically, however, they are not automatically the most likely ones to occur. In the top part of Fig. 5 a schematic view of the lowest IEC's, see also Eq. (4), is shown for two and four ML of Ru. For two ML Ru the ground-state configuration refers to configuration 4 in Table II, for four ML of Ru to configuration 2. In the investigated range of the Ru-spacer thickness antiferromagnetic coupling of the two $Co_{90}Fe_{10}$ slabs via the Ru-spacer occurs only be-

TABLE II. Magnetic configurations investigated in system *D*. The labels 0 and 180 refer to orientations of the magnetization parallel and antiparallel to the surface normal.

Head	0	1	2	3	4	5
$Ni_{80}Fe_{20}$	0	0	0	0	0	0
$(Co_{90}Fe_{10})_5$	0	0	0	0	0	0
$(Cu)_i, i<n/2$	0	0	0	0	0	0
$(Cu)_i, i\geqslant n/2$	0	0	180	0	180	Θ
$(Co_{90}Fe_{10})_5$	0	180	180	180	180	Θ
$(Ru)_i, i<p/2$	0	180	180	180	180	Θ
$(Ru)_i, i\geqslant p/2$	0	0	0	180	180	0
$(Co_{90}Fe_{10})_5$	0	0	0	180	180	0
Vac	0	0	0	180	180	0

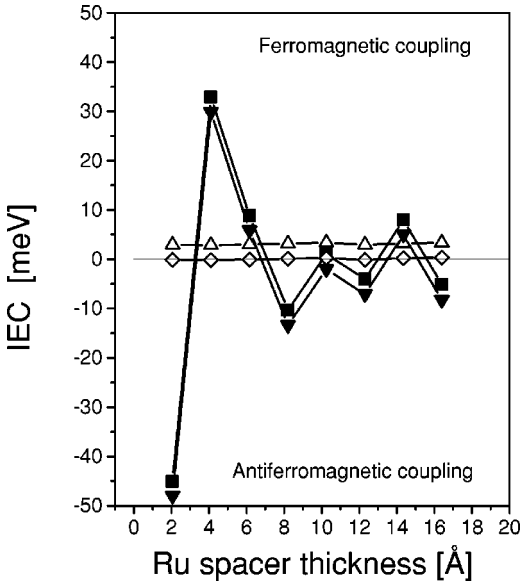

FIG. 4. IEC of partial system *D*, see Table I, with respect to the thickness of the Ru spacer. Full squares and triangles refer to the IEC's corresponding to configurations 1 and 2 in Table II, open triangles and diamonds to configurations 3 and 4. Note that the thickness of the Ru-spacer is given in [Å], 1 ML corresponds to about 2 Å.

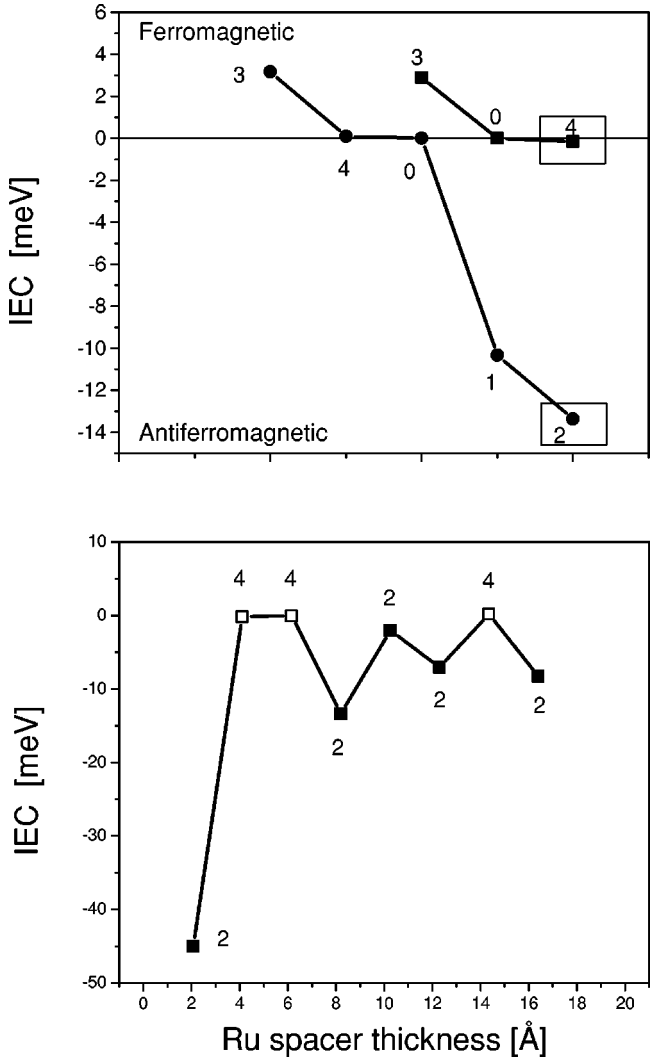

FIG. 5. Top: The lowest configuration dependent IEC's for 2 (squares) and 4 ML (circles) of Ru in partial system *D*. The (collinear) ground-state configuration is marked by a box. Bottom: Oscillations of the IEC corresponding to configurations 2 and 4 with respect to the thickness of the Ru spacer. Note that the thickness of the Ru-spacer is given in [Å], 1 ML corresponds to about 2 Å. The antiparallel configurations, see Table II, are marked explicitly.

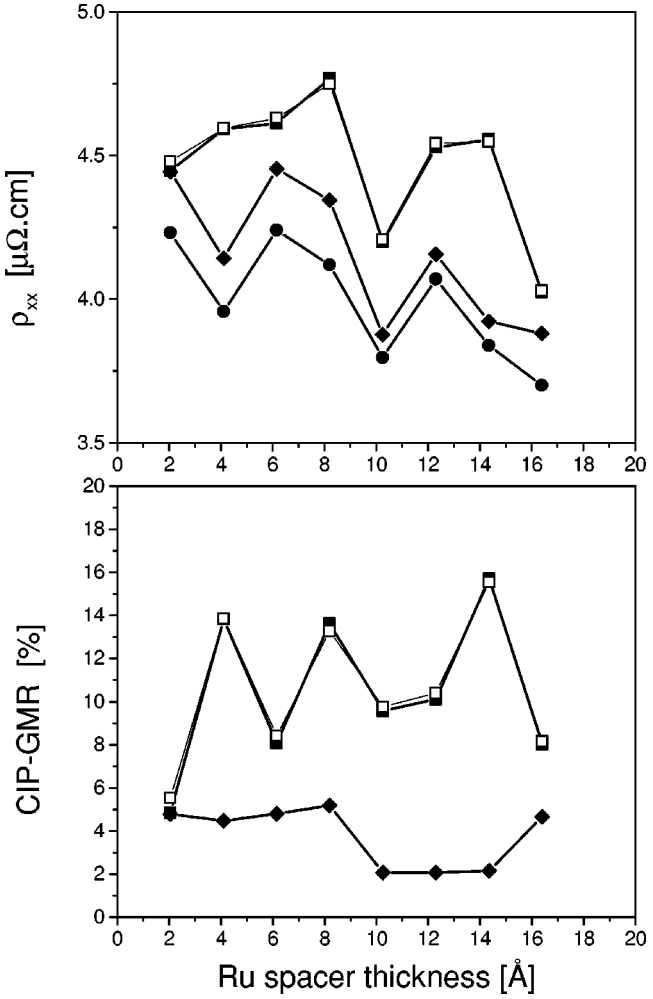

FIG. 6. Resistivities (top) and GMR (bottom) as a function of the thickness of the Ru spacer. Full circles, squares and diamonds refer to configurations 0, 1, and 3, open squares to configuration 2, see also Table II. Note that the thickness is given in [Å], 1 ML corresponds to about 2 Å.

low 3 Å, and inbetween 7 and about 13 Å, in all other cases the coupling between the two $Co_{90}Fe_{10}$ slabs is ferromagnetic, the oscillations with respect to ground states, see lower part of Fig. 5, are between configurations 2 and 4, i.e., between configurations in which either only the two outer $Co_{90}Fe_{10}$ slabs are antiferromagnetically coupled (configuration 4) or all three are antiparallel to each other (configuration 2). It should be recalled that in all figures thicknesses given in Å are with respect to the interlayer spacing of the thick $Ni_{80}Fe_{20}$ film assumed to serve as electron reservoir, i.e., 1 ML corresponds to about 2 Å.

In Fig. 6 the resistivities and the GMR corresponding to some of the configurations listed in Table II are shown. It is interesting to note that the GMR (Fig. 6, bottom) corresponding to configurations 1 and 2 oscillates around 10% with respect to the Ru-spacer thickness, while, e.g., the GMR corresponding to configuration 3 is confined to about 2–4%. In system *A* the corresponding value (10 Å Cu spacer, no Ru cap) is about 19%, in system *B* (Ru cap) the GMR at this particular thickness of the Cu-spacer vanishes completely. This immediately shows that the actual value of the dip in the GMR seen experimentally at about 10 Å obviously depends very much on the kind and quality of the $Co_{90}Fe_{10}$/Ru interface, the origin thereof, however, is primarily related to the Cu spacer. For the reported Ru thickness of 4 Å the present calculation in terms of system *D* predict a GMR of about 4% which compares quite favoritely with the experimentally measured value of about 7%, see also lower part of Fig. 6.

D. Rotational behavior

The final question to be addressed is what changes characterize the IEC, resistivity and the GMR if the orientation of the magnetization is varied continuously from one configuration to another one in the vicinity of a node in the oscilla-

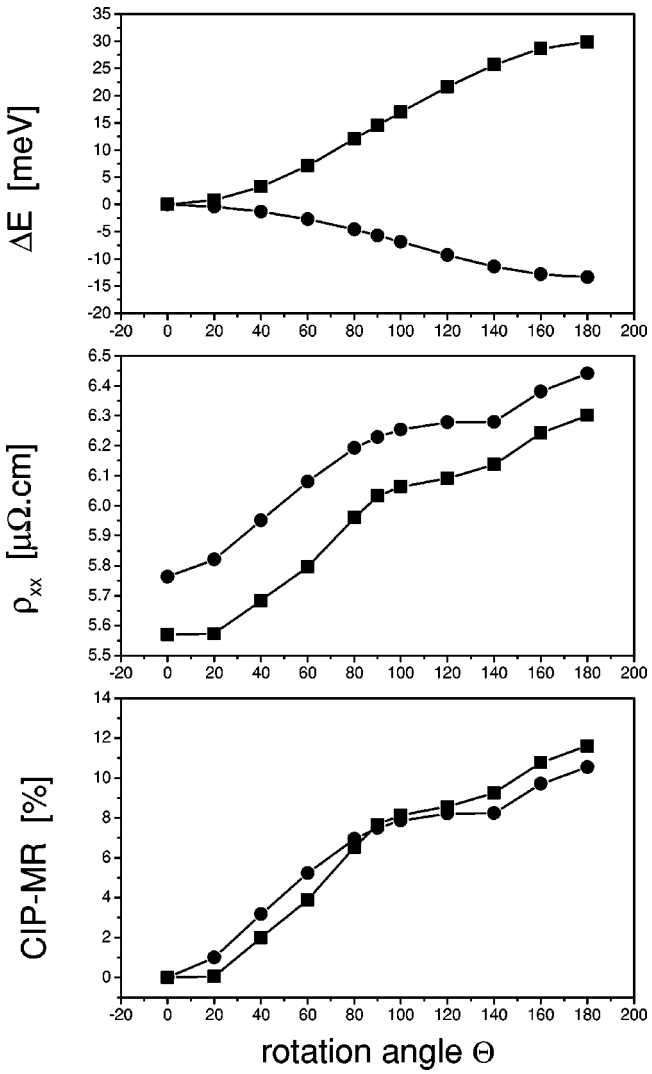

FIG. 7. IEC (top), resistivity (middle), and GMR (bottom) for 2 (squares) and 4 (circles) ML of Ru in system *D* as a function of the rotation angle Θ, see also Table II. For the electric transport properties shown in here an imaginary part of the Fermi energy of 2 mry is used.

tions of the IEC with respect to the number of Cu-spacer layers. From Fig. 1, e.g., one can see that there is such a node in the oscillations at about 10 Å of Cu.

In Fig. 7 the orientation of the magnetization is rotated (rotation angle Θ around an axis $\hat{\mathbf{n}}$ perpendicular to the surface normal) in finite steps from 0° (ferromagnetic configuration) to 180° (configuration 2), see also configuration 5 in Table II. It should be recalled that a function $f(\hat{\mathbf{n}},\Theta)$ can be fitted[14] in terms of the following expansion:

$$f(\hat{\mathbf{n}},\Theta)=f(\hat{\mathbf{n}},0)+\sum_{m=1}^{\infty} a_m(\hat{\mathbf{n}})(1-\cos^m\Theta), \qquad (5)$$

whereby usually two important cases can be distinguished, namely (1) $a_1(\hat{\mathbf{n}}) \gg a_2(\hat{\mathbf{n}})$ and (2) $|a_1(\hat{\mathbf{n}})| \sim |a_2(\hat{\mathbf{n}})|$. In Fig. 7 the functional form of configuration 5 is depicted for two systems of type *D*, namely, for two and four ML of Ru, the parameters $a_1(\hat{\mathbf{n}})$ and $a_2(\hat{\mathbf{n}})$ for these two cases are listed in Table III. While the IEC for both cases mostly shows a $[1-\cos(\Theta)]$ like behavior, the resistivity, as well as the GMR do exhibit considerable deviations from this form: there is a well-pronounced shoulder at 90°. It should be noted that for matters of comparison in both cases (two and four ML of Ru) one and the same type of ''switching'' is shown although only for four ML of Ru configuration 2 is the (collinear) antiparallel ground-state configuration.

TABLE III. Expansion coefficients related to magnetic configuration 2.

Property	$m=2$ a_1	$m=2$ a_2	$m=4$ a_1	$m=4$ a_2
IEC [meV]	14.932	−0.388	−6.681	0.998
ρ_{xx} [$\mu\Omega$ cm]	0.366	−0.096	0.340	−0.127
CIP-MR [%]	5.80	−1.86	5.27	−2.22

IV. DISCUSSION

If one is primarily interested in the IEC then perhaps the question of the asymptotic behavior of this quantity might arise. In order to give a nonspeculative answer to this question, a discrete Fourier transformation of the IEC has to be performed;[15–19] the positions of peaks in the absolute value of this transform then refer to the periods of the oscillation under question. In performing such a discrete Fourier transformation not only the IEC with respect to many layers is needed, but also the so-called preasymptotic regime (spacer thicknesses below 10–15 ML) has to be excluded. Only once well pronounced peaks are found their position can be correlated to Fermi vectors of the bulk spacer material as a kind of asymptotic characterization. Clearly enough Fermi surfaces are well-defined only for three-dimensional periodic systems. For the usual spin-valve systems with Cu-spacer thicknesses below 30 Å it does not make sense to even use the concept of a ''colloquial'' Cu Fermi surface.

One-dimensional discrete Fourier transformations of course apply only to trilayer systems with fixed thicknesses of the magnetic slabs. It is well-known e.g., that by increasing the thickness of one of the magnetic slabs additional oscillations with respect to this thickness parameter set in, see Ref. 18. Furthermore, if the two magnetic slabs consist of different materials different kinds of additional oscillations and/or a bias can be observed. For a system of type D a six-dimensional discrete Fourier transformations would be needed in order to sort out periods of oscillation, since the IEC in principle depends on the thickness of all relevant parts of the spin valve, namely the $Ni_{80}Fe_{20}$, $Co_{90}Fe_{10}$, Cu, and Ru slabs. Since the aim of this study is to investigate the origin of the dips in the GMR such a multidimensional discrete Fourier is well beyond the scope of the present paper.

Pinning effects caused by the AF-part of the experimental system can only be shown by actually including this part in the calculations and comparing again IEC's for different possible configurations.[4] Unfortunately in most spin-valve

systems the energy corresponding to the exchange bias is too small to be described in terms of *ab initio* like methods. Clearly enough the closer one gets to the edge of an antiferromagnetic coupling regime the smaller the magnetic fields have to be in order to achieve switching. The switching itself, however, very well then might not follow a simple $[1-\cos(\Theta)]$ behavior.

V. CONCLUSION

It was shown in this paper that in order to interpret experimental GMR data for a spin-valve as complicated as investigated in here it is extremely useful to partition such a system into significant parts and investigate the physical properties of these partial systems separately. Using this kind of procedure it is found that (1) the major effect of antiferromagnetic coupling for the GMR is— as to be expected— connected with the number of Cu-spacer layers; (2) the actual position of the nodes in the oscillations of the IEC with respect to the number of Cu-spacer layers is unchanged by a rather thin Ru cap; (3) increasing the thickness of the magnetic slabs can increase the antiferromagnetic coupling strength but simultaneously results into a dilution of the GMR effect, and (4) by changing the thickness of the Ru-spacer the dips in the GMR caused by a node in the IEC with respect to the thickness of the Cu-spacer can be monitored. In brief it can be said that in the present case a clear explanation of the experimentally observed ''dips'' in the GMR has been provided; the calculated values for the GMR fit remarkably well to the experimental data.

ACKNOWLEDGMENTS

This work was supported by the Austrian Ministry of Science (Grant No. GZ 45.504), the Hungarian National Science Foundation (Grants Nos. OTKA T030240, T037856) and the RTN network on ''Computational Magnetoelectronics'' (Grant No. HPRN-CT-2000-00143).

[1] E. Y. Tsymbal and D. G. Pettifor, Solid State Phys. **56**, 113 (2001).
[2] S. Jo and M. Seigler, J. Appl. Phys. **91**, 7110 (2002).
[3] C. Blaas, L. Szunyogh, P. Weinberger, C. Sommers, P. M. Levy, and J. Shi, Phys. Rev. B **65**, 134427 (2002).
[4] P. Weinberger, Phys. Rev. B **65**, 014430 (2002).
[5] M. Seigler (private communication).
[6] P. Weinberger, and L. Szunyogh, Comput. Mater. Sci. **17**, 414 (2000).
[7] P. Weinberger, P. M. Levy, J. Banhart, L. Szunyogh, and B. Újfalussy, J. Phys.: Condens. Matter **8**, 7677 (1996).
[8] P. Weinberger, Philos. Mag. B **75**, 509 (1997).
[9] P. Weinberger, C. Blaas, L. Szunyogh, C. Sommers, and P. Entel, Phys. Rev. B **63**, 94 417 (2001).
[10] C. Blaas, L. Szunyogh, P. Weinberger, C. Sommers, and P. M. Levy, Phys. Rev. B **63**, 224408 (2001).
[11] S. H. Vosko, L. Wilk, and M. Nusair, Can. J. Phys. **58**, 1200 (1980).
[12] C. Blaas, P. Weinberger, L. Szunyogh, P. M. Levy, and C. Sommers, Phys. Rev. B **60**, 492 (1999).
[13] C. Blaas, P. Weinberger, L. Szunyogh, C. Sommers, and P. M. Levy, Phys. Rev. B **63**, 224408 (2001).
[14] C. Blaas, P. Weinberger, L. Szunyogh, J. Kudrnovský, V. Drchal, P. M. Levy, and C. Sommers, Eur. Phys. J. B **9**, 245 (1999).
[15] J. Kudrnovský, V. Drchal, C. Blaas, I. Turek, and P. Weinberger, Phys. Rev. Lett. **76**, 3834 (1996).
[16] J. Kudrnovský, V. Drchal, P. Bruno, I. Turek, and P. Weinberger, Phys. Rev. B **54**, R3738 (1996).
[17] J. Kudrnovský, V. Drchal, R. Coehorn M. Šob, and P. Weinberger, Phys. Rev. Lett. **78**, 358 (1997).
[18] J. Kudrnovský, V. Drchal, P. Bruno, I. Turek, and P. Weinberger, Phys. Rev. B **56**, 8919 (1997).
[19] V. Drchal, J. Kudrnovský, P. Bruno, I. Turek, P. H. Dederichs, and P. Weinberger, Phys. Rev. B **60**, 9588 (1999).